第 26 卷　增刊
2009 年 7 月
原子核物理评论
Nuclear Physics Review
Vol. 26, Suppl.
Jul., 2009

Article ID: 1007－4627(2009)Suppl.－0124－05

Recent HERMES Results on DVCS from Proton and Nuclear Targets*

YE Hong-xue, MAO Ya-jun (on behalf of the HERMES Collaboration)
(*School of Physics and State Key Laboratory of Nuclear Physics and Technology,*
Peking University, Beijing 100871, *China*)

Abstract: Spin structure is one of the fundamental subjects in the study of nucleon structure. Recently it is found that Generalized Parton Distributions(GPDs) are related to the total angular momentum carried by partons, which offers a possible solution to the spin puzzle in the first time. We get access to certain GPDs by looking at the azimuthal angle asymmetries attributed to the interference between Deeply Virtual Compton Scattering (DVCS) and Bethe-Heilter processes in HERMES experiment. By measuring the asymmetry with respect to transverse target polarization from proton target, a model-dependent constraint on J_u vs J_d is obtained. Another worldwide unique channel is nuclear DVCS. The preliminary results on asymmetries with respect to beam spin and beam charge are reported.

Key words: GPDs; DVCS; TTSA; nuclear DVCS
CLC number: O572.24　　**Document code**: A

1 Introduction and Motivation

Nucleon spin structure is one of the fundamental topics in the study of nucleon structure. In 1988, the EMC experiment found, quarks total helicity contribution to the proton's spin 1/2 is only $\Delta\Sigma = 0.114 \pm 0.012 \pm 0.026$[1], which means large part of the nucleon spin is unknown. This was called "spin crisis"[2] at that time, and brought in many interests into this field.

In theoretical side, recently a comprehensive description called Generalized Parton Distributions (GPDs)[3-7] became available, which embody Parton Distribution Functions (PDFs) as special cases, and form factors as the first moments[8]. Great interest arose after Ji's relation[8] was found:

$$J^{q,g} = \frac{1}{2} \lim_{t \to 0} \int \mathrm{d}x\, x [H^{q,g}(x, \xi, t) + E^{q,g}(x, \xi, t)] , \tag{1}$$

where $J^{q,g}$ denotes the total angular momentum carried by the quark q or gluon g, and x, ξ and t stand for the usual arguments of GPDs[5]. It means for the first time that GPDs can shed some light on the missing pieces of nucleon spin structure.

In experimental side, Deeply Virtual Compton Scattering(DVCS) process, i.e., the hard exclusive lepton production of a real photon ($ep \to e'p'\gamma$), appears to allow the theoretically cleanest access to GPDs. Several first measurements sensitive to GPD H have already been performed, of either cross section[9, 10], or of cross section asymmetries with respect to beam spin[11] or beam charge[12].

---

* **Received date**: 27 Aug. 2008
* **Foundation item**: National Natural Science Foundation of China(10375002, 10675004)

Biography: Ye hong-xue(1980－), male(Han Nationality), Beijing, China, Ph. D. Student, working on the field of nuclear and particle physics; E-mail: yehx@hep.pku.edu.cn

The more interesting one is with respect to transverse target polarization[13, 14], which can access the GPD E and show the sensitivity to quarks total angular momentum. Another unique channel at HERMES is nuclear DVCS, and right now there is still no experimental results available. DVCS on nuclear targets can not only yield information on nucleon GPDs, but also constrain theoretical models attempting to give a covariant description of nuclear structure, and furthermore provide a better understanding of the nuclear force[15].

The HERES experiment[16] uses the longitudinally polarized 27.6 GeV electron or positron beam of the HERA accelerator at DESY, with a internal gas target which can be changed between Hydrogen, Deuterium, Helium, Nitrogen, etc. In this paper, we will report the recent DVCS results from HERMES collaboration. In Sec. 2, the transverse-target spin asymmetries from proton target are showed, and a model-dependent constraint on J_u vs J_d is obtained; in Sec. 3, the preliminary results on asymmetries with respect to beam spin and beam charge from nuclear targets are reported, and compared to free proton's; finally in Sec. 4, it is a short summary.

2 The Transverse-target Spin Asymmetry

Due to the fact that Bethe-Heilter (BH) process, i. e., the 1st order radiative correction of eN scattering, has the same initial and final states as DVCS process, all physical observables can receive contributions from DVCS, BH, and the interference of these two. In HERMES kinematic region, the DVCS cross section is much smaller than BH, we can only access DVCS process through the interference term. For the unpolarized (U) beam with charge e_l and transversely (T) polarized target with polarization P_T, the interference term is given by[17]:

$$\mathscr{I} \propto - e_l P_T \,\mathrm{Im}(F_2 \mathscr{H} - F_1 \varepsilon) \cdot \sin(\phi - \phi_s)\cos\phi \,, \tag{2}$$

where $F_{1,2}$ is the Pauli, Dirac form factor, and the angles are defined in Fig. 1.

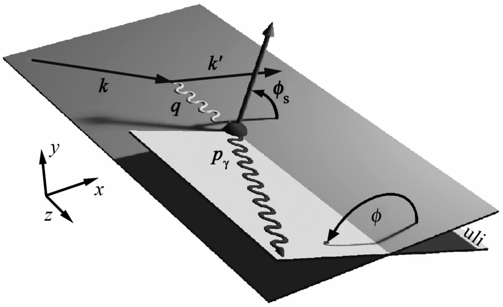

Fig. 1 The kinematic definition for DVCS process in target rest frame. The lepton plane is defined by the incoming and outgoing lepton's 3-momentum k and k'; the production plane is defined by $q = k - k'$ and the real photon's momentum p_γ; the azimuthal angle ϕ is defined by the angle between these two planes, and ϕ_s is defined by the lepton plane and target spin.

By defining the Transverse-target Spin Asymmetry (TTSA) in the form of

$$A_{UT}(\phi, \phi_s) = \frac{\sigma(\phi, \phi_s) - \sigma(\phi, \phi_s + \pi)}{\sigma(\phi, \phi_s) + \sigma(\phi, \phi_s + \pi)} \tag{3}$$

one can see this quantity is sensitive to both GPD H and E according to Eq. 2, and thus has the sensitivity to quark's total angular momentum via Ji's relation.

Transversely polarized proton data from 2002—2005 is analyzed. The integrated luminosities for electron and positron-beam data are approximately 100 pb^{-1} and 70 pb^{-1} respectively. Events are selected if exactly one scattering lepton and one real photon are detected. Because of the low energy and large angle, the recoiling target is not detected by the forward spectrometer. Instead, the missing mass

$$M_X{}^2 = (P_e + P_p - P_{e'} - P_\gamma)^2 \tag{4}$$

is used to select the exclusive sample.

The extracted TTSA amplitudes are shown in Fig. 2. Model calculations on Fig. 2 are based on double-distribution GPD model described in Refs. [5, 18]. Since the Regge-inspired ansatz and without D-term[19] parametrization best describes our Beam Charge Asymmetry data[13], we use this model variant for the TTSA prediction.

Here, the amplitudes of $A_{\mathrm{UT,I}}^{\sin(\phi-\phi_s)\cos\phi}$ is of most interest. Its sensitivity to GPD H and E is confirmed by the theory curves in Fig. 2.

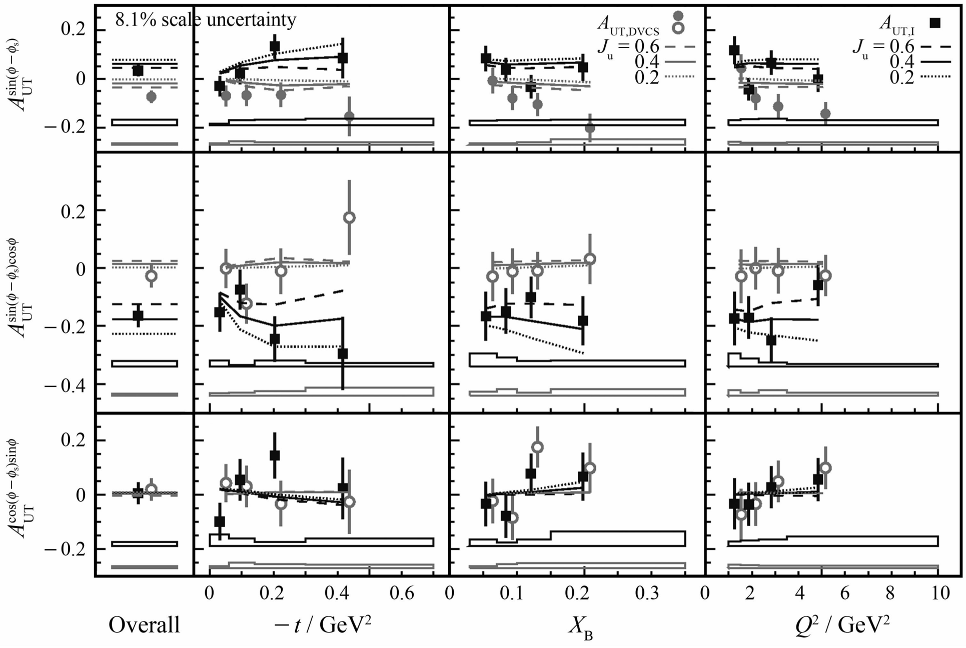

Fig. 2 Asymmetry amplitudes with respect to transverse target spin. The curves are the calculations based on double-distribution GPD model, with 3 different values for the u-quark total angular momentum J_u and fixed d-quark value $J_d = 0$.

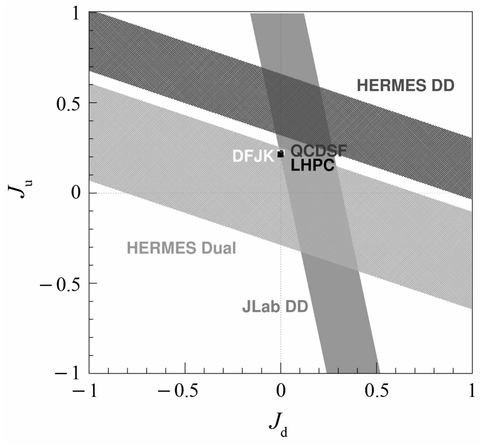

Fig. 3 Model dependent constraints on the u-quark total angular momentum J_u vs d-quark value J_d. The constraints based on HERMES data use the double distribution (HERMES DD) and dual parametrization (HERMES Dual) GPD model. The "JLab DD" band is from the results shown in Ref. [14]. Also shown as small (overlapping) rectangles are the results from lattice gauge theory by different groups.

According to this sensitivity, the J_u and J_d are fit to the measured amplitudes. The area in the (J_u, J_d)-plane in which the reduced $\chi^2 - \chi^2_{\min}$ is less than unity corresponds to a one-standard-deviation constraint on J_u vs J_d, and shown in Fig. 3.

Due to the imperfection of the existing models, these constraints shown in Fig. 3 are quite model dependent. However, such data show the potential to provide quantitative information about the spin content of the nucleon.

3 DVCS Results from Nuclear Target

During nuclear target operating, the target is unpolarized. For longitudinally (L) polarized beam scattering off unpolarized (U) target, we can measured

$$A_C(\phi) = \frac{\sigma^+(\phi) - \sigma^-(\phi)}{\sigma^+(\phi) + \sigma^-(\phi)}, \tag{5}$$

$$A_{LU}(\phi) = \frac{\sigma^{\rightarrow}(\phi) - \sigma^{\leftarrow}(\phi)}{\sigma^{\rightarrow}(\phi) + \sigma^{\leftarrow}(\phi)}, \tag{6}$$

where $A_C(\phi)$ is called as Beam Charge Asymmetry (BCA) and sensitive to the real part of GPD H and

$A_{\text{LU}}(\phi)$ is called as Beam Spin Asymmetry (BSA) and sensitive to the imaginary part of GPD H.

Exclusive production of real photons on nuclear targets involve contributions from coherent and incoherent processes. The former corresponds to the situation when the nuclear target stays intact, while the latter corresponds to the nuclear target breaking up with the photon being emitted by a particular nucleon. Since the coherent process is mostly confined to small t, the squared 4-momentum transfer to the target, it is natural to separate the coherent and incoherent parts using a selection based on t. Of course, a complete separation requires the detecting of the recoiling target, and only (in) coherent-enriched event samples are produced here.

Table 1 Average kinematics and fractions of coherent (incoherent) events in the coherent (incoherent)-enriched sample, shown in the top (bottom) row for each of the targets.

Target	t_{cutoff} /GeV^2	$\langle t \rangle_{\text{rms}}$ /GeV^2	$\langle x_{\text{B}} \rangle_{\text{rms}}$	$\langle Q^2 \rangle_{\text{rms}}$ /GeV^2	Fraction of coh. (incoh.) (%)
H	$-t < 0.033$	−0.018(0.008)	0.070(0.023)	1.81(0.75)	—
	$-t > 0.077$	−0.200(0.120)	0.109(0.059)	2.89(1.62)	—
Kr	$-t < 0.070$	−0.018(0.015)	0.064(0.023)	1.63(0.68)	70
	$-t > 0.067$	−0.200(0.125)	0.108(0.058)	2.84(1.61)	58
Xenon	$-t < 0.078$	−0.018(0.017)	0.062(0.023)	1.60(0.66)	66
	$-t > 0.060$	−0.200(0.126)	0.107(0.058)	2.86(1.63)	56

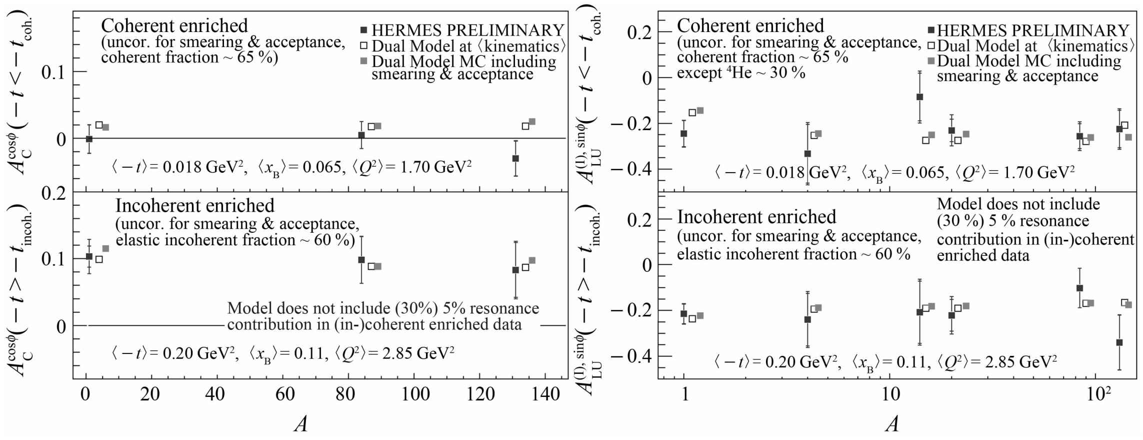

Fig. 4 Leading BCA (top) and BSA amplitude (bottom) in (in-)coherent-enriched samples vs. atomic number. The experimental values are shown as the filled points with double error bars, where the inner one denotes the statistical uncertainty only and the outer one the total experimental uncertainty. Smearing and acceptance effects are not included, but are demonstrated with the Dual-Model simulation: the open boxes show the predicted value at the mean kinematic points, while the filled ones show the extracted asymmetries from a MC production including smearing and acceptance effects.

For each of these two samples, the goal is to compare the results of all targets, and obtain the ratio of the nuclear beam-spin asymmetry to that of hydrogen. Given the kinematic dependence of the asymmetry, this comparison is most meaningful if the data samples for all targets have the same $\langle x_{\text{B}} \rangle$, $\langle Q^2 \rangle$ and $\langle t \rangle$ values. Hence the (lower) upper $|t|$ limit to define the (in-)coherent sample is chosen to obtain the same $\langle t \rangle$ value for all targets, with high but different (in-)coherent purity. The values for Hydrogen, Krypton and Xenon are shown in Table 1 as examples, where one can see

$\langle t \rangle$ is chosen to be -0.018 (-0.20) GeV^2 for the coherent (incoherent-) enriched sample. The variations of $\langle x_\mathrm{B} \rangle$ and $\langle Q^2 \rangle$ between targets remain small.

The measured leading BCA amplitude $A_\mathrm{C}^{\cos\phi}$ and leading BSA amplitudes $A_\mathrm{LU}^{(\mathrm{I}),\ \sin\phi}$ for coherent-enriched and incoherent-enriched samples are shown in Fig. 4 separately. No dependence on atomic number is observed within the experimental uncertainties. The data are compared with two values from the Dual-Model simulation, the difference of which demonstrates instrumental effects. Values of the ratio $A_\mathrm{LU}^{(\mathrm{I}),\ \sin\phi}/A_\mathrm{LU,\ H}^{(\mathrm{I}),\ \sin\phi}$ are also calculated, and their average is found to be 0.91 ± 0.19 for the coherent-enriched sample, and 0.93 ± 0.23 for the incoherent-enriched sample, both of which are compatible with unity.

4 Conclusions

The latest HERMES results on DVCS from proton and nuclear targets are reported. In proton case, the asymmetry with respect to transverse target spin is measured and a model-dependent constraint on J_u vs J_d is obtained. For nuclear DVCS, the asymmetries with respect to beam charge and beam spin are extracted from various targets and compared to the free proton's; in both coherent-enriched and incoherent-enriched regions, the ratio of nuclear BSA to proton is approximately equal to unity.

References:

[1] Ashman J, Badelek B, Baum G, *et al* (The EMC Collaboration). Phys Lett, 1988, B206: 364.

[2] Leader E, Anselmino M. Z Phys, 1988, C41: 239.

[3] Dittes F M, Muller D, Robaschik D, *et al*. Phys Lett, 1988, B209: 325.

[4] Muller D, Robaschik D, Geyeret B, *et al*. Fortschr Phys, 1994, 42: 101.

[5] Goeke K, Polyakov M V, Vanderhaegen M. Prog Part Nucl Phys, 2001, 47: 401.

[6] Belitsky A V, Muller D. Nucl Phys, 2002, A711: 118.

[7] Diehl M. Phys Rept, 2003, 388: 41.

[8] Ji X. Phys Rev Lett, 1997, 78: 610.

[9] Adloff C, Andreev V, Andrieu B, *et al* (H1 Collaboration). Phys Lett, 2001, B517: 47.

[10] Chekanov S, Derrick M, Krakauer D, *et al* (Zeus Collaboration). Phys Lett, 2003, B573: 46.

[11] Airapetian A, Akopov N, Akopov Z, *et al* (HERMES Collaboration). Phys Rev Lett, 2001, 87: 182 001.

[12] Airapetian A, Akopov N, Akopov Z, *et al* (HERMES Collaboration). Phys Rev, 2007, D75: 011 103(R).

[13] Airapetian A, Akopov N, Akopov Z, *et al* (HERMES Collaboration). JHEP, 2008, 06: 066.

[14] Mazouz M, Camsonne A, Camacho C M, *et al* (JLab Hall A Collaboration). Phys Rev Lett, 2007, 99: 242 501.

[15] Polyakov M V. ArXiv: hep-ph/0211444, 2002.

[16] Ackerstaff K, Airapetian A, Akopov N, *et al*. Nucl Instr and Meth, 1998, A417: 230.

[17] Belitsky A V, Mueller D, Kirchner A. Nucl Phys, 2002, B629: 323.

[18] Vanderhaegen M, Guichon P A, Guidal M. Phys Rev, 1999, D60: 094 017.

[19] Polyakov M V, Weis C. Phys Rev, 1999, D60: 114 017.

[20] Guzey V, Teckentrup T. Phys Rev, 2006, D74: 054 027.

[21] Guzey V. ArXiv: hep-ph/08013235, 2008.